Assessment of the sensitivity of VNIR multispectral datasets to detect chloride-bearing deposits on Mars

Vidhya Ganesh Rangarajan[1], Livio L. Tornabene[1], Ernst Hauber[2], Solmaz Adeli[2], and Valentin Bickel[3]

[1]Institute for Earth and Space Exploration/ Department of Earth Sciences, University of Western Ontario, London, Canada (vrangara@uwo.ca)

[2]DLR Institute of Planetary Research, Berlin, Germany

[3]Center for Space and Habitability, University of Bern, Bern, Switzerland

Introduction:

Chloride deposits on Mars serve as important mineralogical markers for the planet's dynamic aqueous past, recording the last phase(s) of liquid water activity (e.g., **[1-3]**). They have often been considered as evidence of extensive reservoirs of surface/subsurface groundwater on early Mars, facilitating chemical sedimentation and perhaps serving as sites for potential biological activity. Most previous campaigns to detect and characterize chloride-bearing deposits have been based on their distinctive thermal infrared spectral signatures **[1-2].** More recently, efforts have also been made to employ machine learning (ML) algorithms to identify "potential chloride-bearing" deposits **[4]**, although validation of such detections has been challenging. This study explores the VNIR spectral characteristics of chlorides, and the capability of currently operational VNIR instruments like the High Resolution Stereo Camera (HRSC) **[5],** the Colour and Stereo Surface Imaging System (CaSSIS) **[6]** and the High Resolution Imaging Science Experiment (HiRISE) **[7]** to spectrally identify/characterize chlorides on Mars, with an aim to potentially serve as a way to validate recent ML-based detections **[4].**

Methods:

In this study, we employ previously utilized and well-known methods like spectral shape and spectral parameter analysis (e.g., **[8-11]**) to assess the chloride-detection capability of HRSC, CaSSIS, and HiRISE. Prior to spectral analysis, an empirical dark-subtraction correction (e.g., **[8-11]**) is also applied to the radiometrically calibrated products to mitigate effects of atmospheric scattering. While this abstract outlines preliminary results from CaSSIS, where applicable, similar inferences may be made for HRSC and HiRISE.

Results and Discussions:

VNIR Spectral Characteristics of Chlorides:

Chlorides generally do not possess any diagnostic features in the VNIR **[12-13]**. Despite that, their VNIR spectral behaviour is still distinctly different from other commonly occurring Martian minerals, as they remain one of the few minerals along with kaolinite and hematite that do not possess a

negative IR slope characteristic of dust/mafic mixtures. **Fig. 1** shows plots of laboratory-based reference spectra **[14]** of hematite, kaolinite and halite and the corresponding spectral response resampled to HRSC, CaSSIS and HiRISE wavelengths. Theoretically, at HRSC and CaSSIS wavelengths, it should be possible to distinguish hematite from kaolinite and chloride-bearing deposits (**Fig. 1**). Alternatively, kaolinite and chloride exhibit similar spectral behaviour, although the RED-IR/RED-NIR slopes for chloride (**Fig. 1c**) are generally steeper than that for kaolinite (**Fig. 1b**). At HiRISE wavelengths however, the three minerals lack distinguishability from each other due to the limited sensitivity of HiRISE band-passes to the RED-IR spectral characteristics of these materials.
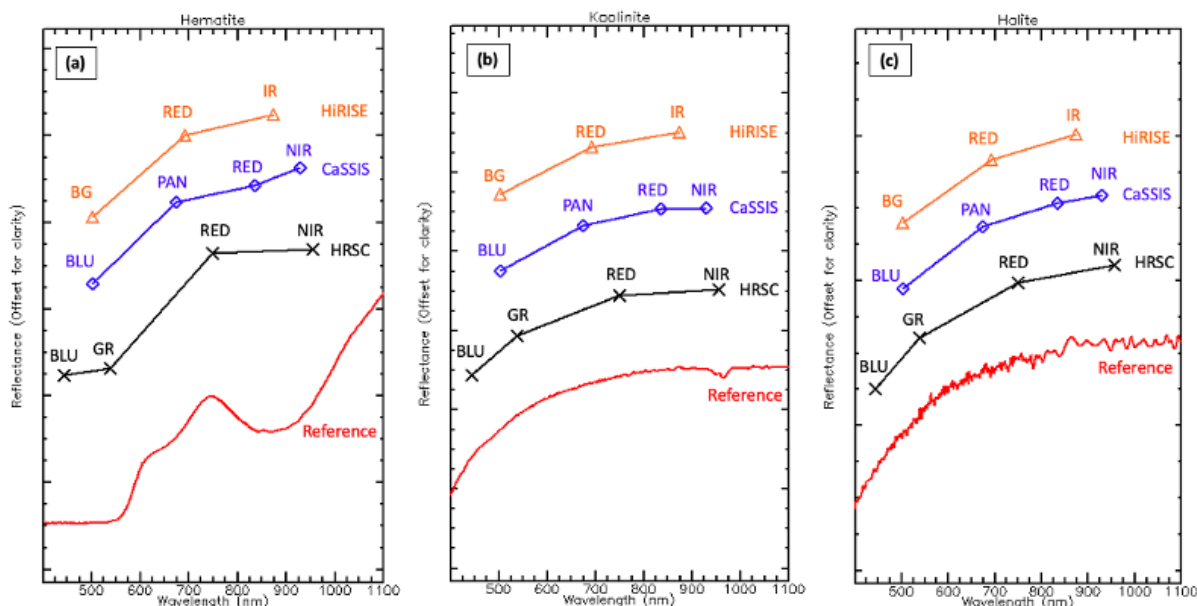
Figure 1. VNIR spectral behaviour of typical laboratory-derived **(a)** hematite, **(b)** kaolinite, and **(c)** halite/chloride bearing materials, and their corresponding spectral responses resampled to HRSC (black spectra with "plus" symbol), CaSSIS (blue spectra with "diamond" symbols) and HiRISE (orange spectra with "triangle" symbols) effective wavelengths. The lab-spectra shown here are obtained from the USGS spectral library **[14]**. We note that at HiRISE wavelengths, it is nearly impossible to confidently distinguish between the three mineral types, while at HRSC and CaSSIS wavelengths, they may be separated to a reasonable extent.
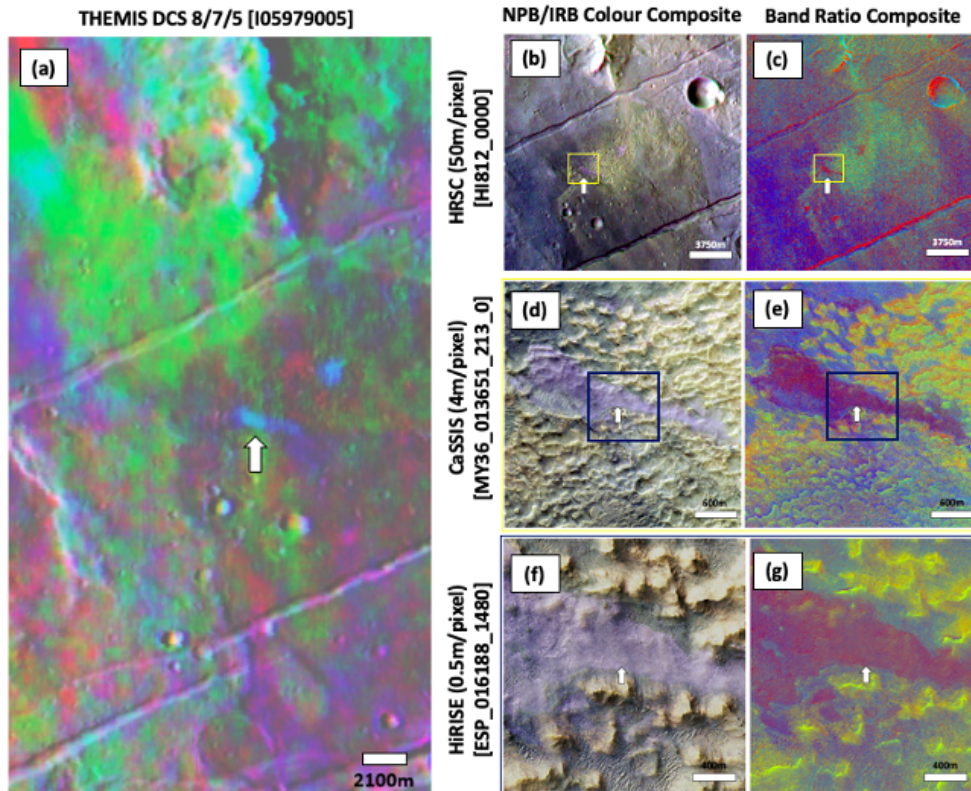
Appearance in Colour and Spectral Band Ratio Composites:

In panchromatic images, like those from the Context Camera **[15]**, chloride-bearing deposits often appear bright and are indistinguishable from other light-toned deposits. However, they show a distinct behaviour in colour infrared multispectral observations. Chlorides have been observed to have a pink-purple hue in colour composites images (e.g., **[1,16]**). **Fig. 2** shows snapshots of four colour composite combinations (NIR-PAN-BLU, RED-PAN-BLU, NIR-RED-BLU and NIR-RED-PAN) of three CaSSIS images showing chloride (**Figs. 2a-2d**), kaolinite (**Figs. 2e-2f**) and hematite-bearing (**Figs. 2i-2l**) deposits respectively. In most CaSSIS colour combinations, the colour of the kaolinite-bearing deposit (**Figs. 2e-2g**) appears pink like that of chloride (**Figs. 2a-2c**). However, the steeper RED-NIR slope observed for chlorides in comparison to kaolinite causes them to be distinguishable in NIR-RED-PAN colour composites, with kaolinites appearing pale yellow (**Fig. 2h**) and chlorides appearing relatively pale pink (**Fig. 2d**). Hematite bearing deposits, on the other hand, appear relatively brown in all four colour composites, allowing them to be distinguished easily from kaolinites and chlorides.
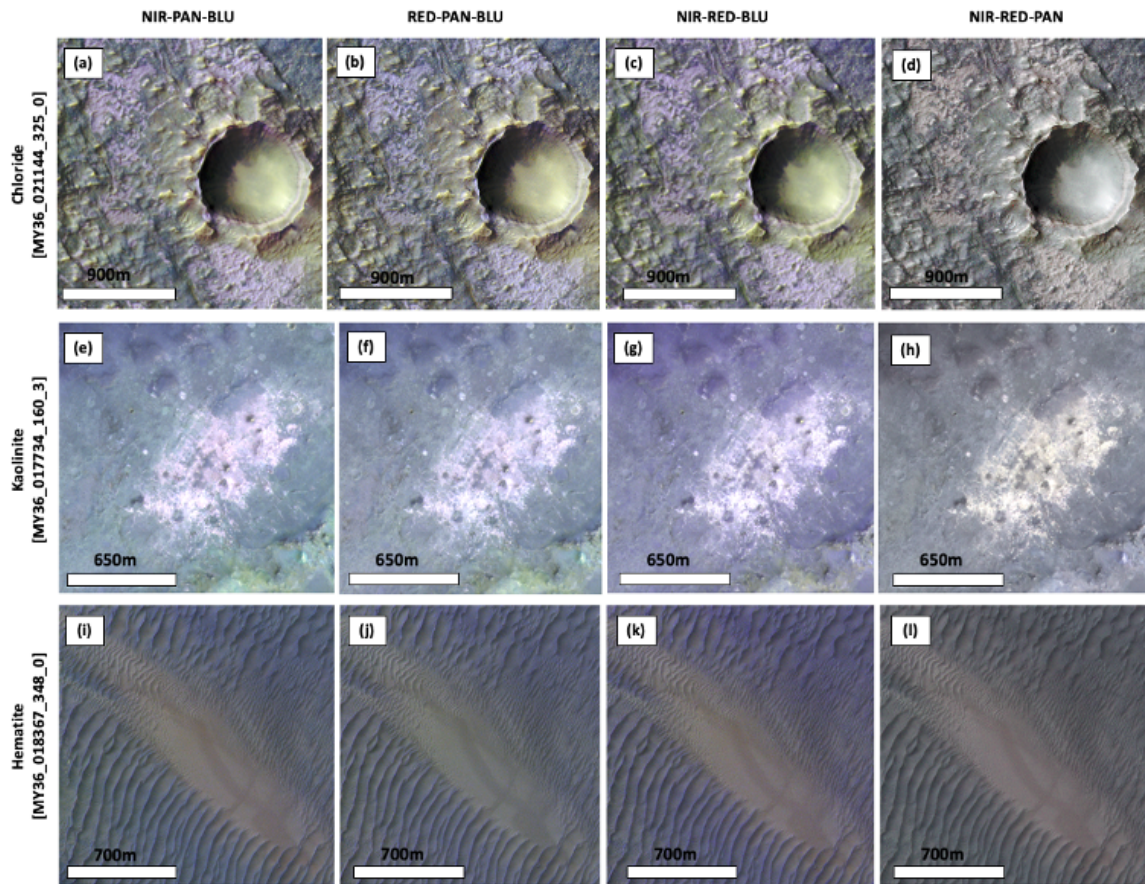
Figure 2. Snapshots of CaSSIS images of **(a-d)** chloride, **(e-h)** kaolinite and **(i-l)** hematite bearing deposits in four colour composite combinations (NIR-PAN-BLU, RED-PAN-BLU, NIR-RED-BLU and NIR-RED-PAN). The CaSSIS images shown here are MY36_021144_325_0, MY36_017734_160_3 and MY36_0018637_348_0 respectively. Chlorides and kaolinite appear pale to bright pink in most colour composites (**Figs. a-c; e-g**) except for the NIR-RED-PAN composite, where chloride appears pale pink (**Fig. d**) while kaolinite appears pale yellow (**Fig. h**). Alternatively, hematite deposits appear relatively brown in all colour composites (**Figs. i-l**).

Since Mars' surface is predominantly covered with dust rich in ferric iron, the effects of the absence of a significant IR slope are further accentuated in the band-ratio space, resulting in distinct appearances of chlorides in colour band ratio composite (CBRC) images (**Fig. 3**). Chlorides typically appear prominently red in CBRCs built by assigning the IR/RED, RED/BLU, and RED/IR spectral ratios to the red, green and blue display channels, respectively. This colour differentiation arises from the positive RED-IR slope of chlorides (**Fig. 1**), which enhances the IR/RED ratio while significantly reducing the value of the RED/BLU spectral parameter. Such CBRCs may also enable global-scale mapping (e.g., **[4]**) at resolutions better than previous chloride surveys **[2].**

THEMIS DCS 8/7/5 [I05979005]

NPB/IRB Colour Composite **Band Ratio Composite**

HRSC (50m/pixel) [HI812_0000]

CaSSIS (4m/pixel) [MY36_013651_213_0]

HiRISE (0.5m/pixel) [ESP_016188_1480]

Figure 3. Snapshots of THEMIS, HRSC, CaSSIS and HiRISE images of the chloride type locality in Terra Sirenum (31.6°S, 206.4°E), characterised by [13]. Panel **(a)** shows the THEMIS DCS 8/7/5 image of the chloride deposit (blue), as characterised by [1]. Panels **(b), (d)** and **(f)** show DS-corrected IR-RED-BLU, NIR-PAN-BLU, and IR-RED-BG colour composites generated from the associated HRSC, CaSSIS and HiRISE image acquisitions of the chloride deposit respectively. Panels **(c), (e)** and **(g)** show corresponding DS-corrected band ratio composites (R: IR/RED; G: RED/BLU; B: RED/IR) built from the HRSC, CaSSIS and HiRISE images respectively. The chloride deposits appear purple to pinkish in the NPB/IRB colour composite, while they appear to have a distinct red colour in the band ratio composites. Note how increase in spatial resolution from THEMIS to HiRISE also adds significant value by resolving the chloride deposit better, thus providing greater details on its texture and morphology.

Spectral Shape Analysis:

It is also observed that performing four-point spectral analyses on DS-corrected CaSSIS images can also serve as means to validate ambiguous chloride deposits. This is described in **Fig. 4** where it is shown that the use of the correction results in arriving at a very close match to the reference halite spectrum in **Fig. 1(c)**. Consequently, this shows that a combination of the spectral methods can provide an efficient means of verifying small-scale deposits with reasonable accuracy.
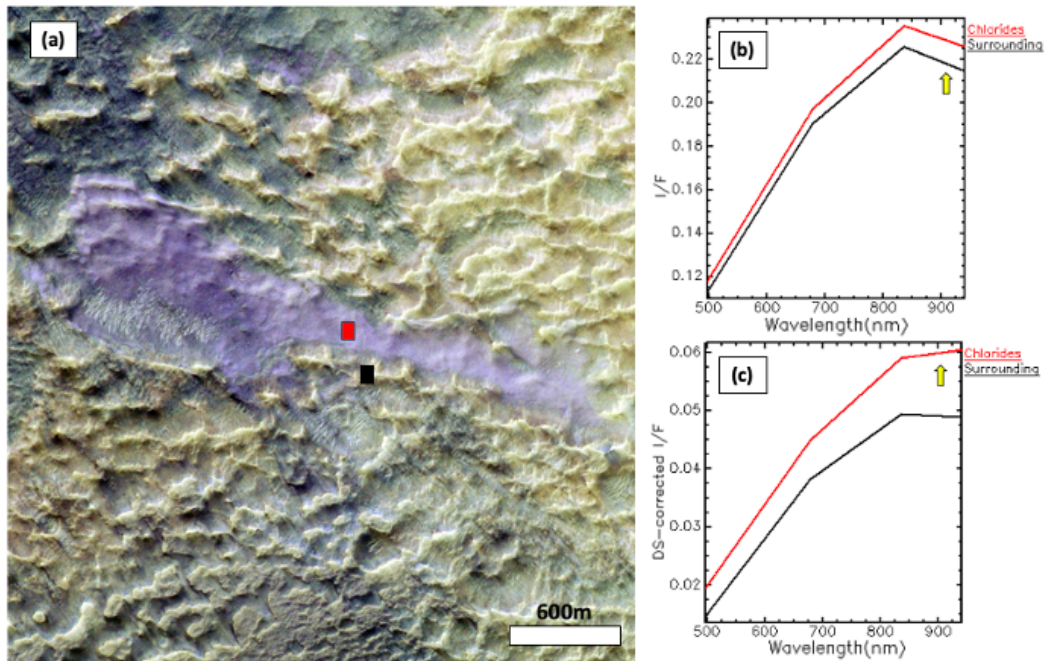
Figure 4. (a) Snapshot of CaSSIS image (MY36_013651_213_0) of the chloride-type locality in Terra Sirenum. Panels **(b)** and **(c)** show spectra extracted from two multi-pixel ROIs – one inside (**red**) and one outside (**black**) the chloride deposit, before and after applying the DS-correction. Note how the DS-correction allows better recovery of the surface spectrum in panel **(c)**, allowing a better spectral match with the reference halite spectrum in **Fig. 1(c)**.

Conclusions:

Our preliminary results show that despite chlorides lacking any VNIR diagnostic absorptions, their unique spectral characteristics allow for them to be characterized with reasonable confidence from multispectral instruments like CaSSIS. While similar spectral characteristics between kaolinite and chlorides are observed, usage of a combination of colour composite maps, CBRCs and spectral shape analysis may aid in separation between the two materials. Integrating these results with topographic information and general geological context may serve as an effective way to enable confident VNIR spectral detection of chloride-bearing deposits, which may be particularly useful to validate results from ML-based surveys **[4].**

Acknowledgements:

References:

[1] Osterloo et al. (2008). *Science*, 319(5870). [2] Osterloo et al. (2010). *JGR*, 115(E10), E10012. [3] Leask and Ehlmann (2022). *AGU Advances*, 3(1).[4] Bickel et al. (2023). *LPSC LIV*, p.1478.[5] Jaumann et al. (2007). *PSS*, 55(7-8). [6] Thomas et al. (2017). *SSR*, 212. [7] McEwen et al. (2007). *JGR*, 112(E5).[8] Tornabene et al. (2018). *SSR*, 214.[9] Tornabene et al. (2022). *LPSC LIII*, p.2330.[10] Rangarajan et al. (2023a). *Icarus*, p.115443.[11] Rangarajan et al. (2023b). *Icarus*, p.115849.[12] Murchie et al. (2009). *JGR*, 114. [13] Viviano et al. (2014). *JGR*, 119.[14] Kokaly et al. (2017). USGS Spectral Library Version 7.[15] Malin et al. (2007). *JGR*, 112(E5).[16] Ye and Glotch (2019). *JGR* 124(2).